Dyes and Pigments 95 (2012) 229–235

Contents lists available at SciVerse ScienceDirect

Dyes and Pigments

journal homepage: www.elsevier.com/locate/dyepig

D–A–D low band gap molecule containing triphenylamine and benzoxadiazole/benzothiadiazole units: Synthesis and photophysical properties

Shaohang Zeng [a], Lunxiang Yin [a], Xueying Jiang [b], Yanqin Li [a,*], Kechang Li [b,*]

[a] School of Chemistry, Dalian University of Technology, Linggong Road 2, Dalian 116024, China
[b] College of Chemistry, Jilin University, 2699 Qianjin Avenue, Changchun 130012, China

ARTICLE INFO

Article history:
Received 13 December 2011
Received in revised form
4 April 2012
Accepted 5 April 2012
Available online 20 April 2012

Keywords:
D–A–D structure
Triphenylamine
Benzoxadiazole
Benzothiadiazole
Donor materials
Photophysical properties

ABSTRACT

Two D–A–D-type low band gap organic dyes based on triphenylamine and benzoxadiazole/benzothiadiazole, 4,7-Bis{5-{4-{2-[4-(N,N-diphenylamino)phenyl]-1-nitrilethenyl}phenyl}-2-thienyl}-2,1,3-benzoxadiazole (**BDNTBX**) and 4,7-Bis{5-{4-{2-[4-(N,N-diphenylamino)phenyl]-1-nitrilethenyl}phenyl}-2-thienyl}-2,1,3-benzothiadiazole (**BDNTBT**) were successfully synthesized. The properties of two compounds were investigated by density functional theory (DFT) calculations, UV–vis absorption spectroscopy, cyclic voltammetry and fluorescence quenching experiment. The calculated ground-state geometries demonstrate intramolecular charge transfer (ICT) occurs in both molecules during the procedure of charge excitation from HOMO to LUMO. From the data in electrochemistry and fluorescence quenching experiments, the molecules reveal lower HOMO energy levels compared with that of P3HT and proper LUMO energy levels to obtain efficient charge separation with PCBM. Two synthesized compounds exhibit broad absorption range covering the whole visible spectral region. These photophysical and electrochemical properties call attention to that our materials are prospective candidates as donor materials for solution-processable organic photovoltaic cells.

© 2012 Elsevier Ltd. All rights reserved.

1. Introduction

Small molecule based organic photovoltaic devices have attracted intensive attention in bulk heterojuction solar cells due to their reproducible preparation, easy functionalization, facile purification and excellent monodisperse [1–4]. Donor(D)–acceptor(A) typed π-conjugated organic materials are widely investigated as active materials in research area of small molecular organic solar cells [5–8] because this design makes it possible to reduce the band gap of the material for broadening the range of absorption and to study the relationship between the variation of donor/acceptor chromophores and their corresponding properties of photophysics and electrochemistry [1,2,9].

The triphenylamine (TPA) unit is considered as a promising donor moiety of D–A typed photovoltaic materials because of its good electron-donating, high hole mobility and well solubility [10–12]. So many kinds of TPA-based molecules have been designed by combining electron-acceptor moiety, such as benzothiadiazole [6,13–16], dicyanovinylene [11,17–19], 1,1,4,4-tetracyanobuta-1,3-diene [20], dicyanomethylenepyran [21], hexafluorocyclopentene [22], sulfonyldibenzene [23], in linear, star-shaped or dendritic structure, and developed as donor materials for organic solar cells with the power conversion efficiency (PCE) of 0.06%–4.3%. Additionally, the utilization of benzothiadiazole (BT) as an accepting moiety and TPA as a donating moiety, in particular by Li and co-workers [6,13–15], is well-studied and successful strategy for synthesizing low band gap donor materials. However, small molecular photovoltaic donor materials using benzoxadiazole (BX) as an alternating acceptor unit is scarcely considered [24], compared with the polymer donor materials [25–29]. Furthermore, BX has been exhibited to lower HOMO energy level of D–A typed materials, which leads to larger open voltage in BHJ solar cells [25–29].

In this paper, we report two new linear, D-π-A-π-D structured organic dyes(Scheme 1) based on TPA as donor units and BT/BX as acceptor units with (4-thienyl)phenyl-ethylene π-conjugated chain between them. In addition, the π-bridge has been designed to connect with nitrile groups, which have been considerably utilized on synthesis of organic dye for the dye-sensitized solar cells [30,31]. The structures of target materials have been designed in order to (i) take advantage of intramolecular charge transfer to reduce band gaps of molecules and to extend the absorption spectrum of them

* Corresponding authors. Tel./fax: +86 411 8498 6040.
E-mail addresses: liyanqin@dlut.edu.cn (Y. Li), likc@jlu.edu.cn (K. Li).

0143-7208/$ – see front matter © 2012 Elsevier Ltd. All rights reserved.
doi:10.1016/j.dyepig.2012.04.001

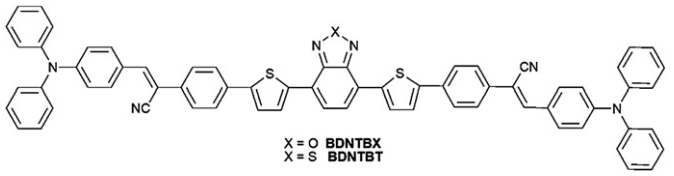

Scheme 1. Chemical structure of **BDNTBX** and **BDNTBT**.

to longer wavelength [1,2], (ii) profit from hole-transport properties and good solution capability of TPA group [10–12], (iii) investigate the relationship between photophysical and electrochemical differences of two molecules and their different acceptor units. Density functional theory (DFT) calculations of two compounds were needed to understand the properties of these conjugated compounds at molecular level. The photophysical properties of new materials have been analyzed by UV–vis absorption spectrum, fluorescence emission spectroscopy and fluorescence quenching experiment with phenyl C_{61} butyric acid methyl (PCBM) which is a soluble fullerene derivative and has been widely used in organic solar cells as an acceptor material. To investigate their properties of electrochemistry, cyclic voltammetry has been applied on these compounds and the results are discussed in relation to the experiment of fluorescence quenching and variation of acceptor moieties.

2. Experimental

2.1. Materials

All reagents were obtained commercially and used without further purification, unless otherwise noted. Toluene and tetrahydrofuran were dried by distillation from metallic sodium/benzophenone under nitrogen atmosphere before use. All reaction carried in an air atmosphere unless otherwise noted.

2.2. Measurements and characterizations

NMR spectra were collected on a Bruker AVANCE II 400-MHz spectrometer (400 MHz for ^{1}H NMR and 100 MHz for ^{13}C NMR), with $CDCl_3$ as solvent and TMS as the internal standard. MS data were measured with MALDI Micro MX spectrometer. UV–vis absorption spectra were recorded on a HP8453 UV–vis spectrophotometer at room temperature using a quartz cuvette as container and chloroform as solvent. For the thin film spectra, the materials were firstly dissolved in chloroform, and drop-casted on glass slide. Fluorescence spectra and fluorescence quenching experiment were carried out with a Shimadzu RF-5301PC spectrofluorometer. Cyclic voltammetry (CV) was performed using a CHI 610D electrochemical workstation from CH Instruments, Inc. On these analyses, the synthesized final molecules were drop-casted on glass-carbon electrode which was used as the working electrode, and Ag/Ag^+ electrode (Ag in 0.1 M $AgNO_3$ solution of MeCN) and platinum wire were used as the reference electrode and the count electrode, respectively. Ferrocene–ferrocenium (Fc/Fc^+) couple was chosen as internal standard. Current–voltage characteristics were carried out using a Keithley 2400 Source Measure Unit under AM 1.5G illumination (100 mW cm^{-2}).

2.3. Synthesis

Details of synthesis of the BT and BX acceptor moieties (compounds 4–**13**) are provided in the supplementary data. NMR spectra of all compounds are available in supplementary materials.

2.3.1. 4-(N,N-Diphenylamino)-benzaldehyde (1)

A solution of palladium acetate (0.045 g, 0.20 mmol), bis(diphenylphosphino)ferrocene (DPPF) (0.28 g, 0.50 mmol) and 4-bromobenzaldehyde (2.8 g, 15 mmol) in dry toluene (100 mL) was stirred under nitrogen atmosphere at room temperature for 30 min. Then, diphenylamine (1.7 g, 10 mmol) and sodium *tert*-butoxide (1.4 g, 15 mmol) were added to the solution and refluxed at 110 °C for 24 h. After being cooled to the room temperature, the reaction mixture was filtered through a short plug of silica gel with ethyl acetate. The organic solvent was evaporated under reduced pressure. The crude product was purified by silica column chromatograghy eluting with petroleum ether/ethyl acetate (v:v, 10:1) to afford compound **1** as an orange solid (1.7 g, 63%); m.p. 128–131 °C (lit [32]., 130–131 °C); ^{1}H-NMR(400 MHz, $CDCl_3$, ppm): δ 9.81 (s, 1H), 7.67 (d, J = 8.8 Hz, 2H), 7.34 (t, 4H), 7.15–7.18 (m, 6H), 7.01 (d, J = 8.8 Hz, 2H).

2.3.2. 2-(4-bromophenyl)-3-[4-(N,N-diphenylamino)phenyl]-acrylonitrile (2)

A solution of sodium hydroxide (0.14 g, 3.6 mmol) in ethanol (5.0 mL) was added to the mixture of compound **1** (0.81 g, 3.0 mmol) and 4-bromobenzyl cyanide (0.71 g, 3.6 mmol) in ethanol (50 mL) at room temperature. After being stirred for 40 h, the yellow solid was filtered and washed by a great amount of water. The resulting solid was dried to afford compound **2** (1.2 g, 89%) without further purification; m.p. 163–164 °C; ^{1}H-NMR(400 MHz, $CDCl_3$, ppm): δ 7.77 (d, J = 8.8 Hz, 2H), 7.49–7.56(m, 4H), 7.40 (s, 1H), 7.32(t, 4H), 7.11–7.17 (m, 6H), 7.04 (d, J = 8.8 Hz, 2H); ^{13}C-NMR (100 MHz, $CDCl_3$, ppm) δ 106.38, 118.46, 120.69, 122.62, 124.57, 125.84, 126.02, 127.18, 129.64, 130.81, 132.13, 134.08, 142.03, 146.51, 150.23; HRMS(MALDI-TOF): 450.0752[M^+] (calcd for $C_{27}H_{19}N_2Br$: 450.0732).

2.3.3. 2-[4-(4,4,5,5-tetramethyl-[1,3,2]dioxaborolan-2-yl)phenyl]-3-[4-(N,N-diphenylamino)phenyl]-acrylonitrile (3)

A solution of compound **2** (2.2 g, 5.0 mmol), bis(pinacolato) diborane (1.5 g, 6.0 mmol), KOAc (1.5 g, 15 mmol), $Pd(PPh_3)_2Cl_2$ (0.18 g, 0.25 mmol) in dry toluene (50 mL) was refluxed at 120 °C under nitrogen atmosphere for 24 h. After being cooled to the room temperature, the mixture was poured into water (100 mL) and the organic layer was separated. The aqueous layer was extracted with dichloromethane (3 × 50 mL) and the combined organic layers were dried over anhydrous Na_2SO_4 and evaporated to dryness. The crude product was purified by silica column chromatograghy eluting with petroleum ether/ethyl acetate (v:v, 5:1) to afford compound **3** (2.0 g, 81%) as an orange solid. m.p. 171–174 °C; ^{1}H-NMR(400 MHz, $CDCl_3$, ppm): δ 7.85 (d, J = 8.4 Hz, 2H), 7.79(d, J = 8.8 Hz, 2H), 7.65 (d, J = 8.4 Hz, 2H), 7.49(s, 1H), 7.32 (t, 4H), 7.10–7.17 (m, 6H), 7.05 (d, J = 8.8 Hz, 2H), 1.36 (s, 12H); ^{13}C-NMR (100 MHz, $CDCl_3$, ppm) δ 24.90, 84.01, 107.58, 118.69, 120.79, 124.44, 124.82, 125.77, 126.32, 129.54, 129.59, 130.83, 135.39, 137.52, 142.18, 146.58, 150.09; HRMS(MALDI-TOF): 498.2490 [M^+] (calcd for $C_{33}H_{31}BN_2O_2$: 498.2479).

2.3.4. 4,7-Bis{5-{4-{2-[4-(N,N-diphenylamino)phenyl]-1-nitrilethenyl}phenyl}-2-thienyl}-2,1,3-benzoxadiazole (BDNTBX)

2 mL of ethanol and 4 mL of 2 M aqueous Na_2CO_3 were added to the solution of compound **9** (0.22 g, 0.50 mmol), compound **3** (0.50 g, 1.0 mmol) and $Pd(PPh_3)_4$ (0.058 g, 0.050 mmol) in 8 mL of toluene under nitrogen atmosphere. Then the mixture was refluxed at 110 °C for 48 h. After being cooled to the room temperature, the mixture was poured into water (50 mL) and the organic layer was separated. The aqueous layer was extracted with chloroform (3 × 50 mL) and the combined organic layers were dried over anhydrous Na_2SO_4 and evaporated to dryness. The crude product was purified by silica column chromatograghy eluting with

chloroform/AcOH (v:v, 50:1) to afford compound BDNTBX as a dark brown solid (0.26 g, 56%); m.p. 283–287 °C; ^{1}H-NMR(400 MHz, $CDCl_3$, ppm): δ 8.13 (d, J = 2.8 Hz, 2H), 7.82 (d, J = 8.4 Hz, 4H), 7.65–7.74 (m, 8H), 7.65 (s, 2H), 7.48(s, 4H), 7.33 (t, 8H), 7.12–7.18 (m, 12H), 7.06 (d, J = 8.4 Hz, 4H); HRMS(MALDI-TOF): 1024.2979 [M^+] (calcd for $C_{68}H_{44}N_6OS_2$: 1024.3018).

2.3.5. 4,7-Bis{5-{4-{2-[4-(N,N-diphenylamino)phenyl]-1-nitrilethenyl}phenyl}-2-thienyl}-2,1,3-benzothiadiazole (BDNTBT)

2 mL of ethanol and 4 mL of 2 M aqueous Na_2CO_3 were added to the solution of compound **13** (0.23 g, 0.50 mmol), compound **3** (0.50 g, 1.0 mmol) and $Pd(PPh_3)_4$ (0.058 g, 0.050 mmol) in 8 mL of toluene under nitrogen atmosphere. Then the mixture was refluxed at 110 °C for 48 h. After being cooled to the room temperature, the mixture was poured into water (50 mL) and the organic layer was separated. The aqueous layer was extracted with chloroform (3 × 50 mL) and the combined organic layers were dried over anhydrous Na_2SO_4 and evaporated to dryness. The crude product was purified by silica column chromatograghy eluting with petroleum ether/chloroform (v:v, 1:10) to afford compound BDNTBT as a dark brown solid (0.39 g, 75%); m.p. 288–293 °C; ^{1}H-NMR(400 MHz, $CDCl_3$, ppm): δ 8.13 (d, J = 2.8 Hz, 2H), 7.91 (s, 2H), 7.80(d, J = 8 Hz, 4H), 7.68–7.76 (m, 8H), 7.47(s, 4H), 7.33 (t, 8H), 7.11–7.18 (m, 12H), 7.05 (d, J = 8 Hz, 4H); ^{13}C-NMR (100 MHz, $CDCl_3$, ppm) δ107.03, 118.63, 120.82, 124.46, 124.60, 125.43, 125.77, 126.15, 126.36, 127.44, 128.29, 128.75, 129.59, 130.77, 134.23, 134.33, 139.19, 141.24, 144.62, 146.58, 150.06, 152.55; HRMS(MALDI-TOF): 1040.2700 [M^+] (calcd for $C_{68}H_{44}N_6S_3$: 1040.2790).

3. Results and discussion

3.1. Synthesis and characterization

The synthetic routes of **BDNTBX** and **BDNTBX** are shown in Scheme 2. Compound 4-(N,N-diphenylamino)-benzaldehyde (**1**) is prepared by the Buchwald–Hartwig C–N coupling reaction of diphenylamine and 4-bromobenzaldehyde. Next, Knoevenagel condensation of compound **1** and 4-bromobenzyl acetonitrile was taken place to obtain compound **2** in 89% yields. The compound **2** was borylated with bis(pinacolato)diborane by Miyaura borylation to give donor block **3** in high yield of 81%. The synthesis of acceptor blocks of **9** and **13** were prepared in several steps according to literature procedures: benzofurazan-N-oxide (**4**) [33], 2,1,3-benzoxadiazole (**5**) [34], 4,7-dibromo-2,1,3-benzoxadiazole (**6**) [27], tributyl(thiophen-2-yl)stannane (**7**) [35], 4,7-bis(thiophen-2-yl)-2,1,3-benzoxadiazole (**8**) [27], 4,7-bis(5-bromothiophen-2-yl)-2,1,3-benzoxadiazole (**9**) [27], 2,1,3-benzothiadiazole (**10**) [36], 4,7-dibromo-2,1,3-benzothiadiazole (**11**) [36], 4,7-bis(thiophen-2-yl)-2,1,3-benzothiadiazole (**12**) [35], 4,7-bis(5-bromothiophen-2-yl)-2,1,3-benzothiadiazole (**13**) [35]. **BDNTBX** and **BDNTBT** were synthesized by Suzuki coupling reaction with yields of 56% and 75%, respectively. The chemical structures of two designed compounds

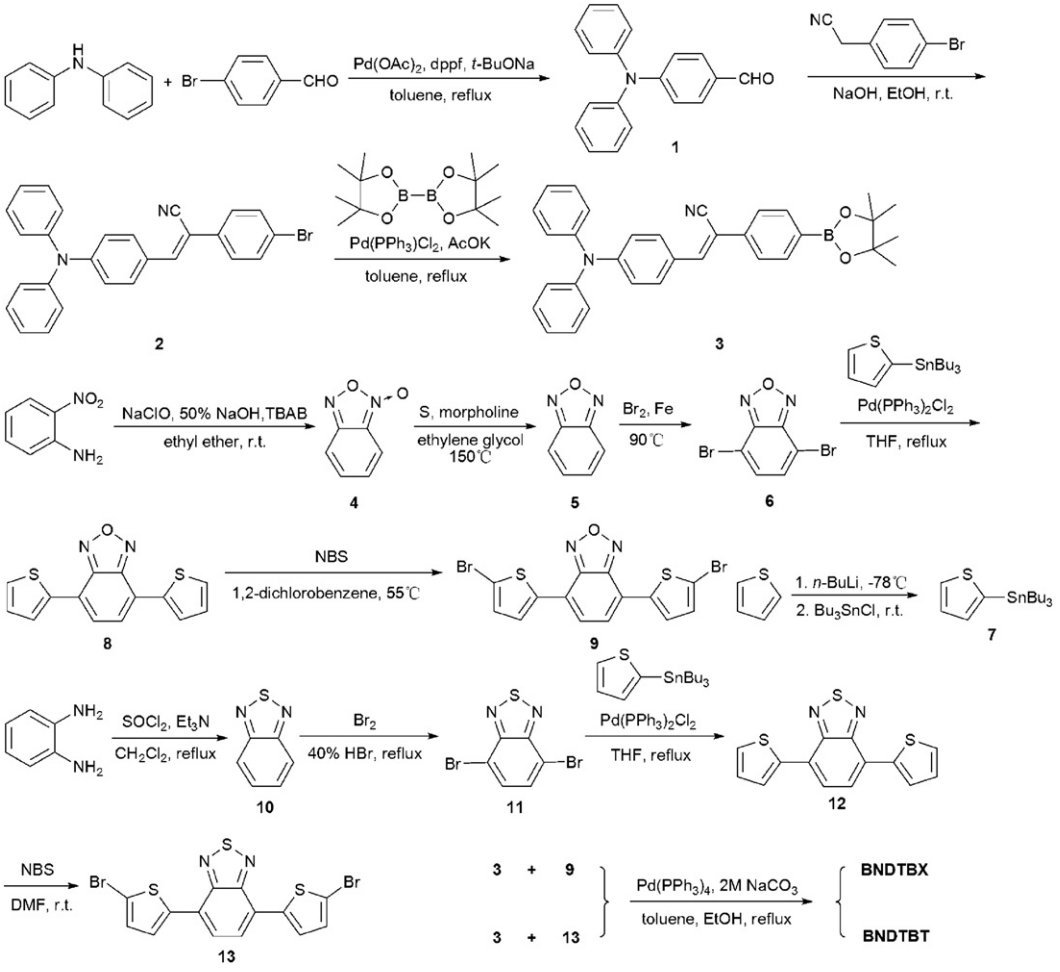

Scheme 2. Synthetic routes of **BDNTBX** and **BDNTBT**.

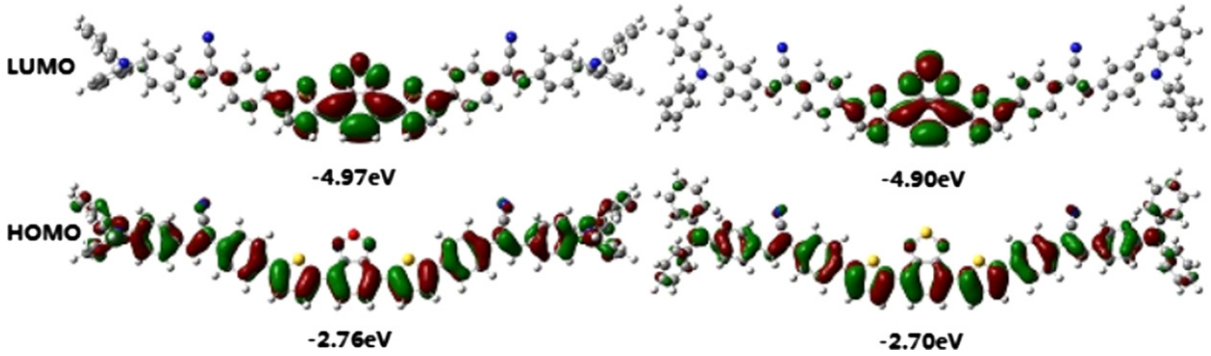

Fig. 1. Molecular orbital surfaces of the HOMO and LUMO of **BDNTBX** (left) and **BDNTBT** (right) obtained at B3LYP/6-31G(d) level.

were identified by MALDI-TOF HRMS and NMR spectra. Both of synthesized molecules have good solubility in common solvent, such as chloroform, chlorobenzene and 1,2-dichlorobenzene, at room temperature to satisfy the requirement on fabrication of photovoltaic device.

3.2. Theoretical calculation

The ground-state geometries and electronic structures of **BDNTBX** and **BDNTBT** were calculated with Gaussian 09 software, using density functional theory (DFT) based on the Becke's three-parameter gradient-corrected functional (B3LYP) with a polarized 6-31G(d) basis [37]. The geometries and the electron-density distribution of the highest occupied molecular orbit (HOMO) and the lowest unoccupied molecular orbit (LUMO) of ground-state optimized structures are illustrated in Fig. 1. The DFT calculated HOMO and LUMO energies are summarized in Table 1. The calculation results of two molecules demonstrate that the central BX and BT moieties constitute a large conjugated planar structure with their two adjacent thienyl units, and both of the structures appear a slight non-planar structure from the phenyls connected on thienyl units to the two triphenylamine moieties located at the end of molecules. In two compounds, electron density of the HOMO delocalizes over the entire molecules, while that of the LUMO distributes on the acceptor unites of BX and BT, indicating that in the process of being excited from HOMO to LUMO energy levels, a charge transfers from the electron-donating N atom of the TPA units to the central BX or BT acceptor moieties. The calculated HOMO and LUMO energy levels of ground-state optimized geometry for compound BDNTBX are −4.97 eV and −2.76 eV, respectively. The theoretical band gap of BDNTBX is 2.21 eV, estimated by using the differences between the HOMO and LUMO energies. For BDNTBT, the HOMO and LUMO energy levels and theoretical band gap are −4.90 eV, −2.71 eV and 2.19 eV, respectively. The calculation results demonstrate that both of the HOMO and LUMO energy levels of BDNTBX are effectively stabilized by the BX-acceptor units, suggesting the stronger electron-withdraw abilities of BX than that of BT.

3.3. Optical properties

The normalized UV–vis absorption spectra of two studied materials in $CHCl_3$ and in film are inllustrated in Fig. 2. For comparison, the corresponding maximum absorption peaks (λ_{max}) and optical band gap (E_g^{opt}) are listed in Table 1. Both of compounds exhibit strong absorption in wavelength range from 300 to 600 nm in solution on account of their D–A–D molecular structure connected by conjugated bridge. The λ_{max} of compounds **BDNTBX** in solution are observed at 433 nm and 510 nm. The first peak is due to the π–π^* transition of the molecule and the second one can be assigned to the intramolecular charge transfer transition(ICT) between donor unit and acceptor moiety. In comparison with BDNTBX, the absorption peaks of **BDNTBT** are at 433 nm and 501 nm in $CHCl_3$. The slight blue shift of ICT peaks of **BDNTBT** indicates that BX moiety has stronger electron withdrawing effect than BT unit to increase charge transfer between donors and acceptors in molecules.

The absorption spectra in films show generally similar pictures to those in chloroform, but the range of absorption is broadened. Compared with absorption spectra in solution, both of molecules in solid films have a slight red shift of λ_{max} (5 nm for **BDNTBX**, 18 nm for **BDNTBT**), revealing intermolecular π–π interaction and aggregation in solid state. The optical band gap (E_g^{opt}) calculated from onset of absorption edges in the films are 1.83 eV for **BDNTBX** and 1.89 eV for **BDNTBT**, for the reason that enhanced ICT transition of **BDNTBX** results broader the absorption spectral range. In solution, photoluminescence (PL) spectra of compound **BDNTBX** reveals an emission maximum (λ_{max}^{PL}) peaked at 631 nm with excitation wavelength of 510 nm and that of **BDNTBT** displays λ_{max}^{PL} at 630 nm with excitation wavelength located at 500 nm.

3.4. Electrochemical properties

Cyclic voltammetry (CV) measurements of **BDNTBX** and **BDNTBT** were performed in anhydrous acetonitrile with 0.1 M tetrabutylammonium trtrafluoroborate (Bu_4NBF_4) as supporting electrolyte at scan rate of 50 mV s^{-1} under nitrogen atmosphere, in order to determine their HOMO and LUMO energy levels. Using ferrocene–ferrocenium (Fc/Fc^+) couple (E_{FOC} = 0.48 eV *versus* vacuum level) as internal standard, the HOMO energy levels, LUMO energy levels and the electrochemical band gaps (E_g^{ec}) of two molecules were calculated from onset oxidation potentials (E_{ox}) and onset reduction potentials (E_{red}) according to the following equations [38,39]:

Table 1
Optical, electrochemical and DFT calculated properties of **BDNTBX** and **BDNTBT**.

Compound	UV–vis absorption spectra			Cyclic voltammetry					DFT calculation	
	λ_{max}^{sol}/nm	λ_{max}^{film}/nm	E_g^{opt}/eV	E_{ox}/V	HOMO/eV	E_{red}/V	LUMO/eV	E_g^{ec}/eV	HOMO/eV	LUMO/eV
BDNTBX	433,510	431,515	1.83	0.67	−5.42	−1.14	−3.61	1.81	−4.97	−2.76
BDNTBT	433,501	434,519	1.89	0.72	−5.47	−1.18	−3.57	1.90	−4.90	−2.71

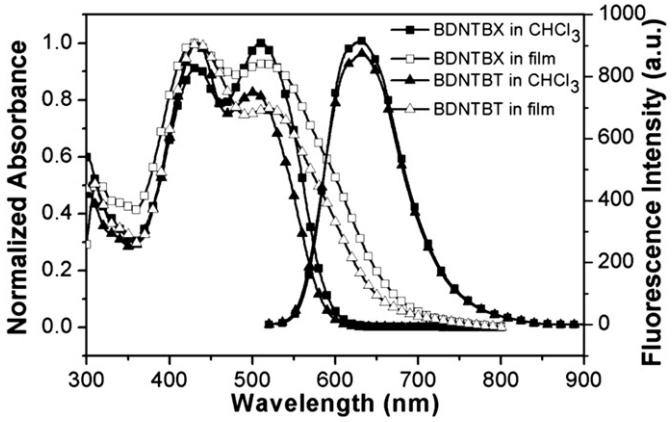

Fig. 2. Fluorescence and UV–vis absorption spectra of **BDNTBX** and **BDNTBT** in chloroform (1.0×10^{-5} M) and in film.

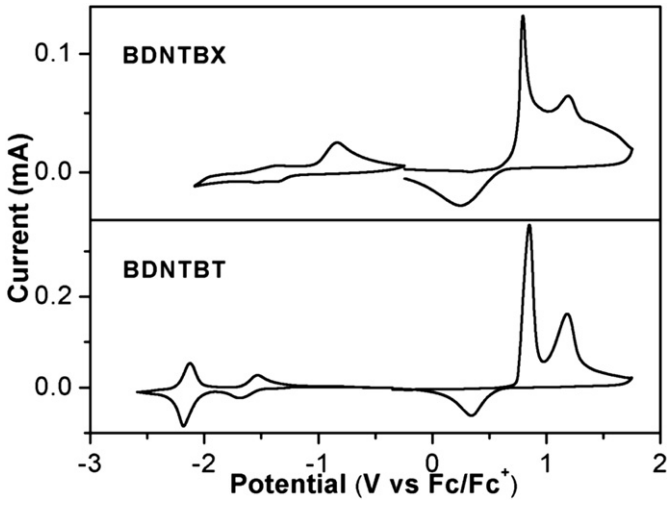

Fig. 3. Cyclic voltammetry curves of **BNDTBX** (top) and **BNDTBT** (bottom) film on glass carbon electrode in 0.1 M Bu_4NBF_4/MeCN solution at scan rate of 50 mV/s.

$$\text{HOMO} = -(E_{ox} - E_{1/2}^{\text{ferrocene}} + 4.8)\ \text{eV}$$

$$\text{LUMO} = -(E_{red} - E_{1/2}^{\text{ferrocene}} + 4.8)\ \text{eV}$$

$$E_g^{ec} = \text{LUMO} - \text{HOMO}$$

where E_{ox} and E_{red} are the measured onset potentials relative to Ag/Ag^+. $E_{1/2}^{\text{ferrocene}} = 0.05$ V *versus* Ag/Ag^+.

The CV curves of two studied molecules are shown in Fig. 3 as a comparison and the results of electrochemical measurements and calculated energy levels are summarized in Table 1. On the anodic scan, two molecules showed irreversible onset oxidation potentials of 0.67 V for **BDNTBX** and 0.72 V for **BDNTBT**. In contrast, the cathodic scan exhibited a reduction of onset potentials of −1.14 V for **BDNTBX** and −1.18 V for BDNTBT. From the Table 1, the band gaps (E_g^{cv}) of **BDNTBX** and **BDNTBT** are estimated to be about 1.81 eV and 1.90 eV, respectively, which are in good agreement with the optical band gaps. For compound **BDNTBX**, the substitution of stronger electron-withdraw group BX results in a lower LUMO level of −3.61 eV, a higher HOMO level of −5.42 eV and a narrower band gap compared with those of **BDNTBT**. In addition, the HOMO energy level of donor materials of small molecular BHJ solar cells plays an important role on high device efficiency, because the difference between the HOMO level of donor materials and the LUMO level of acceptor materials has a linear relationship with the V_{oc} of BHJ solar cells. The relative lower HOMO levels of both molecules (−5.42 eV for **BDNTBX**, −5.47 eV for **BDNTBT**) than that of the polymer donors, such as P3HT (−4.99 eV, Figure S14 in supplementary materials, P3HT was purchased from Sigma-Alderich Inc.), lead them to be favored for increasing the V_{oc} when utilizing two materials as the donors in BHJ solar cell with PCBM as the acceptor.

3.5. Mechanism of photoinduced charge separation

According to electrochemical properties of **BDNTBX** and **BDNTBT**, both of them have potential to generate photoinduced charge separation process with PCBM since that the LUMO energy levels of two molecules are higher than that of PCBM (−4.3 eV) over 0.3 eV, which is required to guarantee the efficient charge separation at interface of donor materials and PCBM [40]. To investigate the charge separation process, the fluorescence quenching experiments were carried out and shown in Fig. 4. The fluorescence of two donor materials was gradually quenched as the concentration of PCBM was increased in $CHCl_3$. This phenomenon suggests an efficient photoinduced charge separation process of synthesized donor molecules with acceptor material PCBM. Furthermore, at low quencher concentrations, the dependences of fluorescence intensity on the concentration of PCBM are linear in conformity with the Stern–Volmer equation [41–44]:

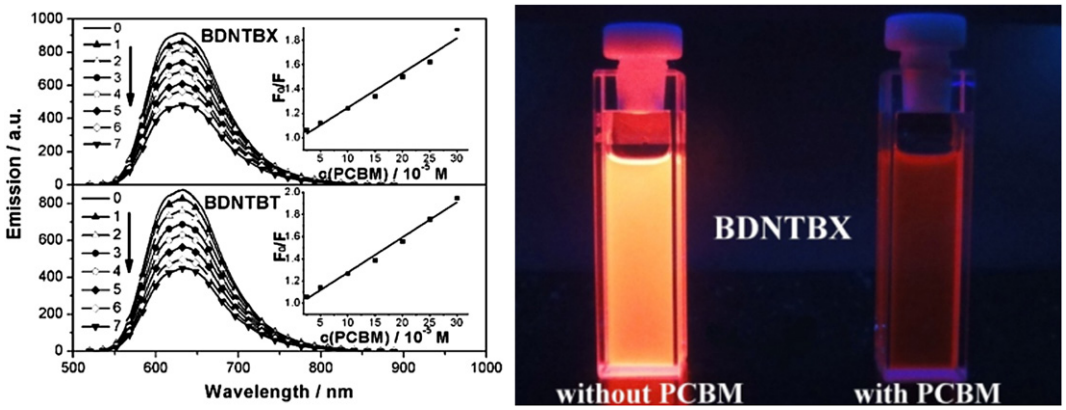

Fig. 4. Emission spectra (left) of **BDNTBX** and **BDNTBT** (1.0×10^{-5} M) in $CHCl_3$ with increasing concentration of $PC_{61}BM$ ($\times 10^{-5}$ M): 0.0 (0), 2.5 (1), 5.0 (2), 10.0 (3), 15.0 (4), 20.0 (5), 25.0 (6), 30.0 (7). The insets are Stern–Volmer quenching plots for both compounds respectively. Fluorescence of BDNTBX without and with PCBM in $CHCl_3$ under irradiation (365 nm) on the setting of Panasonic DSC-TX1 camera (right).

$$D_{TM} + A_{PCBM} \xrightleftharpoons{h\nu} D_{TM}^{*} + A_{PCBM} \quad (1)$$

$$D_{TM}^{*} + A_{PCBM} \rightleftharpoons [D_{TM}^{*}, A_{PCBM}] \quad (2)$$

$$[D_{TM}^{*}, A_{PCBM}] \rightleftharpoons [D_{TM}^{+}, A_{PCBM}^{-}] \quad (3)$$

$$[D_{TM}^{+}, A_{PCBM}^{-}] \rightleftharpoons D_{TM}^{+} + A_{PCBM}^{-} \quad (4)$$

Scheme 3. Mechanism for photoinduced charge separation of synthesized donor molecules (D_{TM}) with acceptor PCBM (A_{PCBM}): (1) excitation of D_{TM} by incident photon; (2) diffusion of exciton in solution to form an encounter pair; (3) transfer of excited electron from D_{TM} to A_{PCBM}; (4) charge separation.

$$F_0/F = 1 + K_{SV}\cdot[C]$$

in which F_0 and F represent the fluorescence intensity in the absence and present of PCBM, respectively, K_{SV} is the quenching constant, and $[C]$ is the concentration of PCBM. The K_{SV} values of **BDNTBX** and **BDNTBT** are 2.85×10^3 M^{-1} and 3.17×10^3 M^{-1}, respectively.

The mechanism for photoinduced charge separation [40,44] is illustrated in Scheme 3. The quenching of fluorescence according to following procedure: (1) under incident ray, the electron on the HOMO energy level of donor molecule was photoexcited to the LUMO energy level to generate a Coulomb-correlated electron-hole pair, an exciton (D_{TM}^{*}); (2) in the solution condition, the photoexcitation of donor diffused to interface of PCBM to form encounter pair ($[D_{TM}^{*}, A_{PCBM}]$); (3) the exciton transfer from the LUMO energy level of donor materials to that of PCBM to form a geminate pair ($[D_{TM}^{+}, A_{PCBM}^{-}]$); (4) the geminate pair dissociate from each other, causing fluorescence quenching.

3.6. Preliminary investigation of photovoltaic properties

In order to exploit the photovoltaic properties of two dyes, we fabricated devices with structure (I) ITO/PEDOT-PSS/BDNTBT:PCBM/Al and structure (II) ITO/PEDOT-PSS/BDNTBX:PCBM/Al. Fig. 5 shows the Current–voltage characteristics of the cells under illumination of one sun AM 1.5G. (100 mW cm^{-2}). The device (I) exhibited an open-circuit voltage (Voc) of 0.60 V, short-circuit current density (Jsc) of 2.86 mA cm^{-2}, fill factor (FF) of 0.29, and power conversion efficiency (PCE) of 0.50%. The device (II) exhibited an open-circuit voltage (Voc) of 0.58 V, short-circuit current density (Jsc) of 2.39 mA cm^{-2}, fill factor (FF) of 0.24, and power conversion efficiency (PCE) of 0.33%. The preliminary investigation suggests that optimization of the device composition, morphology, and annealing are needed, thus further work is under investigation.

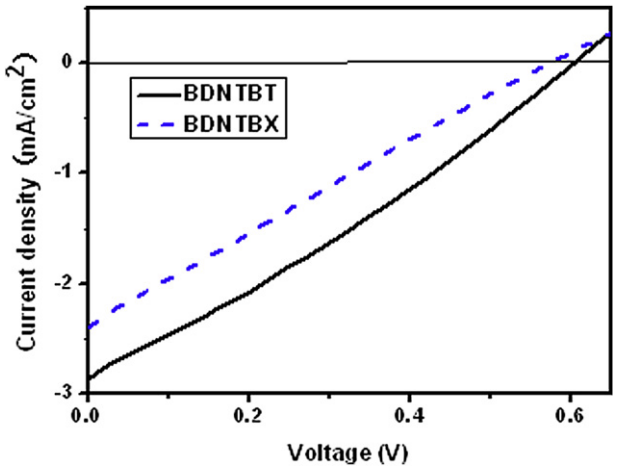

Fig. 5. Current–voltage characteristics for PV cells with structure ITO/PEDOT-PSS/BDNTBT:PCBM/Al (solid line) and ITO/PEDOT-PSS/BDNTBX:PCBM/Al (dash line) under illumination of one sun AM 1.5G (100 mW cm^{-2}).

4. Conclusions

In this work, we have successfully synthesized two new low-band-gap linear D-π-A-π-D organic molecules containing triphenylamine as donor moiety and benzoxadiazole or benzothiadiazole as acceptor moiety. By introducing a BX unit as an alternative acceptor of BT in design of molecules, **BDNTBX** presents a narrower band gap and a lower LUMO energy level compared with those of **BDNTBT**, indicating that BX has better electron-withdrawing capability than BT. DFT calculations of these compounds reveal intramolecular charge transfer from the electro-donating TPA moieties to the central acceptor units. Both of compounds in films show a broad and strong absorption band in the range of 300–700 nm covering nearly whole visible region. The cyclic voltammetry data of them imply that our molecules have lower-lying HOMO energy levels (−5.42 eV for **BDNTBX**, −5.47 eV for **BDNTBT**) comparing with P3HT, which has a HOMO energy level of around 5.0 eV. Furthermore, the fluorescence quenching experiment reveal an efficient photoinduced charge separation mechanism with PCBM. These photophysical and electrochemical properties call attention to that our materials are prospective candidates as donor materials for high-performance solution-processable organic solar cells. Further experiments of fabrication and optimization of solar cells are underway in our laboratory.

Acknowledgment

We thank the NSFC (21102013, 20803030), the Dalian Committee of Science and Technology (2011J21DW001), the SRF for ROCS-Chinese State Education Ministry (No. 201001438, No. 201001439), the Fundamental Research Funds for the Central Universities (DUT11LK20), and the Specialized Research Fund for the Doctoral Program of Higher Education of China (No. 20090041120017) for financial support.

Appendix A. Supplementary material

supplementary material related to this article can be found online at doi:10.1016/j.dyepig.2012.04.001.

References

[1] Walker B, Kim C, Nguyen TQ. Small molecule solution-processed bulk heterojunction solar cells. Chem Mater 2011;23:470–82.
[2] Li YW, Guo Q, Li ZF, Pei JN, Tian WJ. Solution processable D–A small molecules for bulk-heterojunction solar cells. Energy Environ Sci 2010;3:1427–36.
[3] Roncali J. Molecular bulk heterojunctions: an emerging approach to organic solar cells. Acc Chem Res 2009;42:1719–30.
[4] Lloyd M, Anthony J, Malliaras G. Photovoltaics from soluble small molecules. Mater Today 2007;10:34–41.
[5] Walker B, Tamayo AB, Dang XD, Zalar P, Seo JH, Garcia A, et al. Nanoscale phase separation and high photovoltaic efficiency in solution-processed, small-molecule bulk heterojunction solar cells. Adv Funct Mater 2009;19:3063–9.
[6] Shang HX, Fan HJ, Liu Y, Hu WP, Li YF, Zhan XW. A solution-processable star-shaped molecule for high-performance organic solar cells. Adv Mater 2011;23:1554–7.
[7] Loser S, Bruns CJ, Miyauchi H, Ortíz RP, Facchetti A, Stupp SI, et al. A naphthodithiophene-diketopyrrolopyrrole donor molecule for efficient solution-processed solar cells. J Am Chem Soc 2011;133:8142–5.
[8] Yin B, Yang LY, Liu YS, Chen YS, Qi QJ, Zhang FL, et al. Solution-processed bulk heterojunction organic solar cells based on an oligothiophene derivative. Appl Phys Lett 2010;97:023303.

[9] Cheng YJ, Yang SH, Hsu CS. Synthesis of conjugated polymers for organic solar cell applications. Chem Rev 2009;109:5868–923.
[10] Shirota Y. Organic materials for electronic and optoelectronic devices. J Mater Chem 2000;10:1–25.
[11] Roquet S, Cravino A, Leriche P, Alévêque O, Frère P, Roncali J. Triphenylamine–thienylenevinylene hybrid systems with internal charge transfer as donor materials for heterojunction solar cells. J Am Chem Soc 2006;128:3459–66.
[12] Ning ZJ, Tian H. Triarylamine: a promising core unit for efficient photovoltaic materials. Chem Commun 2009;37:5483–95.
[13] He C, He QG, Yi YP, Wu GL, Bai FL, Shuai ZG, et al. Improving the efficiency of solution processable organic photovoltaic devices by a star-shaped molecular geometry. J Mater Chem 2008;18:4085–90.
[14] Shang HX, Fan HJ, Shi QQ, Li S, Li YF, Zhan XW. Solution processable D–A–D molecules based on triphenylamine for efficient organic solar cells. Sol Energy Mater Sol Cells 2010;94:457–64.
[15] Deng D, Yang Y, Zhang J, He C, Zhang MJ, Zhang ZG, et al. Triphenylamine-containing linear D–A–D molecules with benzothiadiazole as acceptor unit for bulk-heterojunction organic solar cells. Org Electron 2011;12:614–22.
[16] Zhu WH, Wu YZ, Wang ST, Li WQ, Li X, Chen J, et al. Organic D-A-π-A solar cell sensitizers with improved stability and spectral response. Adv Funct Mater 2011;21:756–63.
[17] Cravino A, Leriche P, Alévêque O, Roquet S, Roncali J. Light-emitting organic solar cells based on a 3D conjugated system with internal charge transfer. Adv Mater 2006;18:3033–7.
[18] Zhang J, Deng D, He C, He YJ, Zhang MJ, Zhang ZG, et al. Solution-processable star-shaped molecules with triphenylamine core and dicyanovinyl endgroups for organic solar cells. Chem Mater 2011;23:817–22.
[19] Wang B, Wang YC, Hua JL, Jiang YH, Huang JH, Qian SX, et al. Starburst triarylamine donor–acceptor–donor quadrupolar derivatives based on cyano-substituted diphenylaminestyrylbenzene: tunable aggregation-induced emission colors and large two-photon absorption cross sections. Chem Eur J 2011;17:2647–55.
[20] Leliège A, Blanchard P, Rousseau T, Roncali J. Triphenylamine/tetracyanobutadiene-based D–A–D pi-conjugated systems as molecular donors for organic solar cells. Org Lett 2011;13:3098–101.
[21] Zhang J, Wu GL, He C, Deng D, Li YF. Triphenylamine-containing D–A–D molecules with (dicyanomethylene)pyran as an acceptor unit for bulk-heterojunction organic solar cells. J Mater Chem 2011;21:3768–74.
[22] Fan CB, Yang P, Wang XM, Liu G, Jiang XX, Chen HZ, et al. Synthesis and organic photovoltaic (OPV) properties of triphenylamine derivatives based on a hexafluorocyclopentene "core". Sol Energy Mater Sol Cells 2011;95:992–1000.
[23] Li KP, Qu JL, Xu B, Zhou YH, Liu LJ, Peng P, et al. Synthesis and photovoltaic properties of novel solution-processable triphenylamine-based dendrimers with sulfonyldibenzene cores. New J Chem 2009;33:2120–7.
[24] Lin ZH, Bjorgaard J, Yavuz AG, Kose ME. Low band gap star-shaped molecules based on benzothia(oxa)diazole for organic photovoltaics. J Phys Chem C 2011;115:15097–108.
[25] Nie WY, MacNeill CM, Li Y, Noftle RE, Carroll DL, Coffin RC. A soluble high molecular weight copolymer of benzo[1,2-b:4,5-b′]dithiophene and benzoxadiazole for efficient organic photovoltaics. Macromol Rapid Commun 2011;32:1163–8.
[26] Hoven CV, Dang XD, Coffin RC, Peet J, Nguyen TQ, Bazan GC. Improved performance of polymer bulk heterojunction solar cells through the reduction of phase separation via solvent additives. Adv Mater 2010;22:E63–6.
[27] Blouin N, Michaud A, Gendron D, Wakim S, Blair E, Neagu-Plesu R, et al. Toward a rational design of poly(2,7-carbazole) derivatives for solar cells. J Am Chem Soc 2008;130:732–42.
[28] Padhy H, Huang J-H, Sahu D, Patra D, Kekuda D, Chu CW, et al. Synthesis and applications of low-bandgap conjugated polymers containing phenothiazine donor and various benzodiazole acceptors for polymer solar cells. J Polym Sci, Part A: Polym Chem 2010;48:4823–34.
[29] Bijleveld JC, Shahid M, Gilot J, Wienk MM, Janssen RAJ. Copolymers of cyclopentadithiophene and electron-deficient aromatic units designed for photovoltaic applications. Adv Funct Mater 2009;19:3262–70.
[30] Hagfeldt A, Boschloo G, Sun LC, Kloo L, Pettersson H. Dye-sensitized solar cells. Chem Rev 2010;110:6595–663.
[31] Mishra A, Fischer MK, Bäuerle P. Metal-free organic dyes for dye-sensitized solar cells: from structure: property relationships to design rules. Angew Chem Int Ed Engl 2009;48:2474–99.
[32] Tang XL, Liu WM, Wu JS, Lee CS, You JJ, Wang PF. Synthesis, crystal structures, and photophysical properties of triphenylamine-based multicyano derivatives. J Org Chem 2010;75:7273–8.
[33] Dyall LK. Oxidative cyclizations. VII. Cyclization of 2-substituted anilines with alkaline hypohalite. Aust J Chem 1984;37:2013–26.
[34] Kondyukov IZ, Karpychev YV, Belyaev PG, Khisamutdinov GK, Valeshnii SI, Smirnov SP, et al. Sulfur as a new low-cost and selective reducing agent for the transformation of benzofuroxans into benzofurazans. Russ J Org Chem 2007;43:635–6.
[35] Kim J, Park SH, Cho S, Jin Y, Kim J, Kim I, et al. Low-bandgap poly(4H-cyclopenta[*def*]phenanthrene) derivatives with 4,7-dithienyl-2,1,3-benzothiadiazole unit for photovoltaic cells. Polymer 2010;51:390–6.
[36] Dasilveiraneto B, Lopes A, Ebeling G, Goncalves R, Costa V, Quina F, et al. Photophysical and electrochemical properties of π-extended molecular 2,1,3-benzothiadiazoles. Tetrahedron 2005;61:10975–82.
[37] Frisch MJ, Trucks GW, Schlegel HB, Scuseria GE, Robb MA, Cheeseman JR, et al. Gaussian 09, revision A1. Wallingford CT: Gaussian, Inc.; 2009.
[38] Li ZT, Zhang Y, Holt AL, Kolasa BP, Wehner JG, Hampp A, et al. Electrochromic devices and thin film transistors from a new family of ethylenedioxythiophene based conjugated polymers. New J Chem 2011;35:1327–34.
[39] Yu CY, Chen CP, Chan SH, Hwang GW, Ting C. Thiophene/phenylene/thiophene-based low-bandgap conjugated polymers for efficient near-infrared photovoltaic applications. Chem Mater 2009;21:3262–9.
[40] Thompson BC, Fréchet JM. Polymer-fullerene composite solar cells. Angew Chem Int Ed Engl 2008;47:58–77.
[41] Wang J, Wang DL, Miller EK, Moses D, Bazan GC, Heeger AJ. Photoluminescence of water-soluble conjugated polymers: origin of enhanced quenching by charge transfer. Macromolecules 2000;33:5153–8.
[42] Wang J, Wang D, Miller EK, Moses D, Heeger AJ. Static and dynamic photoluminescence (PL) quenching of polymer: quencher systems in solutions. Synth Met 2001;119:591–2.
[43] Wang J, Wang D, Moses D, Heeger AJ. Dynamic quenching of 5-(2′-ethylhexyloxy)-*p*-phenylene vinylene (MEH-PPV) by charge transfer to a C60 derivative in solution. J Appl Polym Sci 2001;82:2553–7.
[44] Zhao TY, Liu ZX, Song YB, Xu W, Zhang DQ, Zhu DB. Novel diethynylcarbazole macrocycles: synthesis and optoelectronic properties. J Org Chem 2006;71:7422–32.